Supplementary Information 1: Preservation

A total of three fossil (*Campanile giganteum*) and one modern (*Campanile symbolicum*) specimens were studied to assess the suitability of *Campanile* gastropods for paleoseasonality reconstructions. Of the studied specimens, one specimen (E1) is approximately 120 mm long and, contains a total of 11 whorls. The outside of the E1 contains numerous boreholes and the ostracum is worn out. The broken distal edge of E1 suggests that it represents the apex of a larger specimen. Two other specimens, E2 (230 mm long, 17 whorls) and E3 (383 mm long, 15 whorls) were less affected by predatory boring. All three *Campanile giganteum* shells are missing the very tip of the apex, which means that the very first growth time is not recorded. Interpretation of the stable isotope curves and growth modelling suggests that the missing part of these shells likely represents no more than a few months (see **Fig. 4** and **Fig. 6** in main text). In order to illustrate this, records in **Fig. 4** are plotted such that the first 6 growth months contain no data. This period is likely an overestimation of the amount of time missing from the apices of the shells. Specimen **C2** was acquired fully intact, measuring 130 mm, counting 22 whorls and only suffered a few boreholes and some wear on the apex of the shell. High-resolution color scans of cross sections through all shells as well as pictures of the shells documenting their preservation are found in **Fig. S1**.
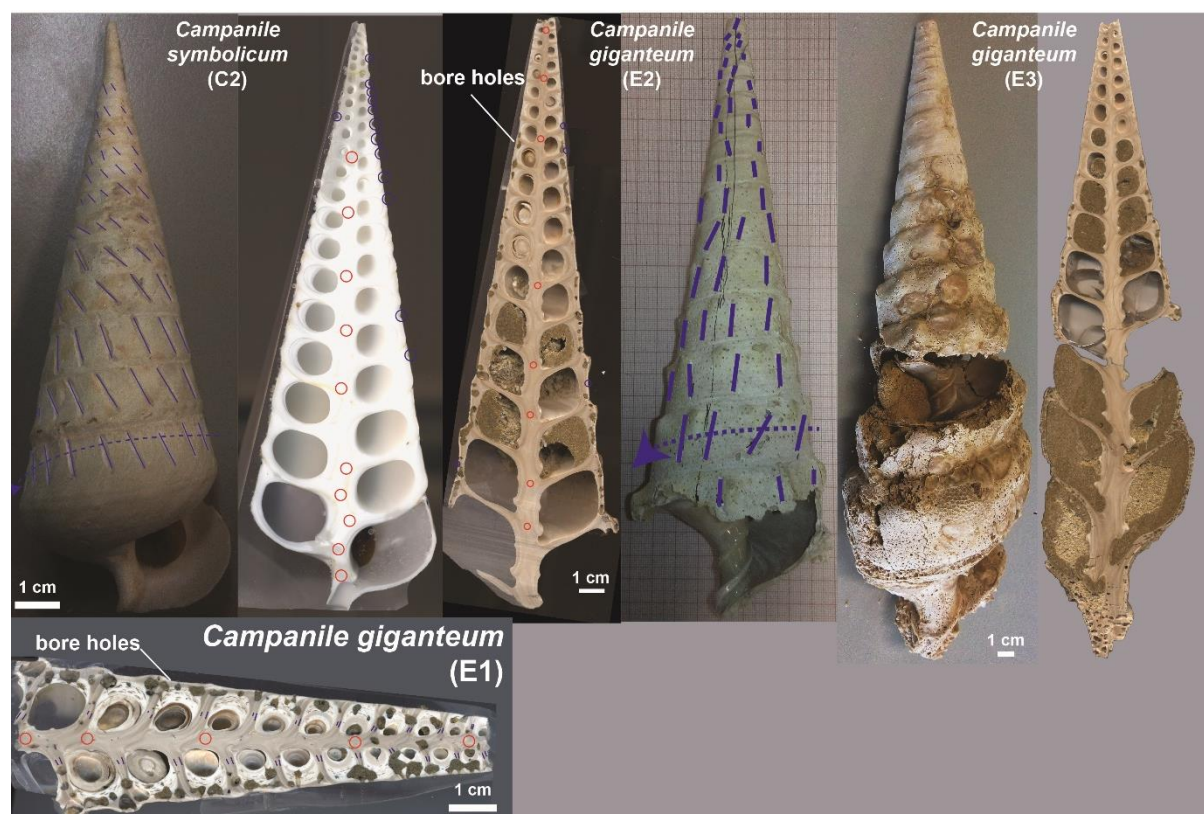
Fig. S1: *Overview of pictures and scans of the outside and the cross sections of the four specimens used in this study. Scale bars below images are 1 centimeter long.*

In order to assess the preservation of original aragonite in the shells of *Campanile giganteum*, we applied Scanning Electron Microscopy on shell fragments originating from several parts (outer shell wall, columella, inside of whorl and secondary aragonite deposited inside the whorl) of **E1**. Shell fragments were mechanically broken to expose fresh fracture surfaces, which were sputter-coated with carbon before introduced into a JEOL JSM-IT300 (JEOL, Ltd, Tokyo, JP) Scanning Electron Microscope. The JEOL JSM-IT300 is equipped with a tungsten filament electron source and was operated in low-vacuum mode while collecting secondary electron images of mineral structures in the various parts of the shell. Fracture

surfaces of the shell fragments were imaged at 33x to 4500x magnification (see scale bars in **Fig. S2**) to visualize individual aragonite crystals in shell layers. The quality of sample preservation was assessed based on the preservation scale suggested by Cochran et al. (2010). SEM images show that the fossil specimens of *Campanile giganteum* contain well-preserved aragonite in their inner shell layers. The fibrous crossed-lamellar structure of the aragonite (best viewed in **Fig S2B**) closely resembles that found in modern marine gastropods (e.g. Dauphin et al., 1989; Taylor and Reid, 1990). High magnification images show that individual aragonite prisms are not visually affected by dissolution or recrystallisation and would score high on the "Preservation Index" scale by Cochran et al. (2010). The outermost layer of aragonite is nacreous and contains well preserved columnar tablets visible in fractural cross sections (see **Fig S2C-D**), attesting to the shell's excellent preservation. Lower resolution images show that areas surrounding burrows contain secondary minerals presumably precipitated from the fluid after boring by the parasitic organism as well as detrital material (**Fig S2A**). The effect of burrowing on original shell preservation was shown to be very local and these areas were avoided during sampling.
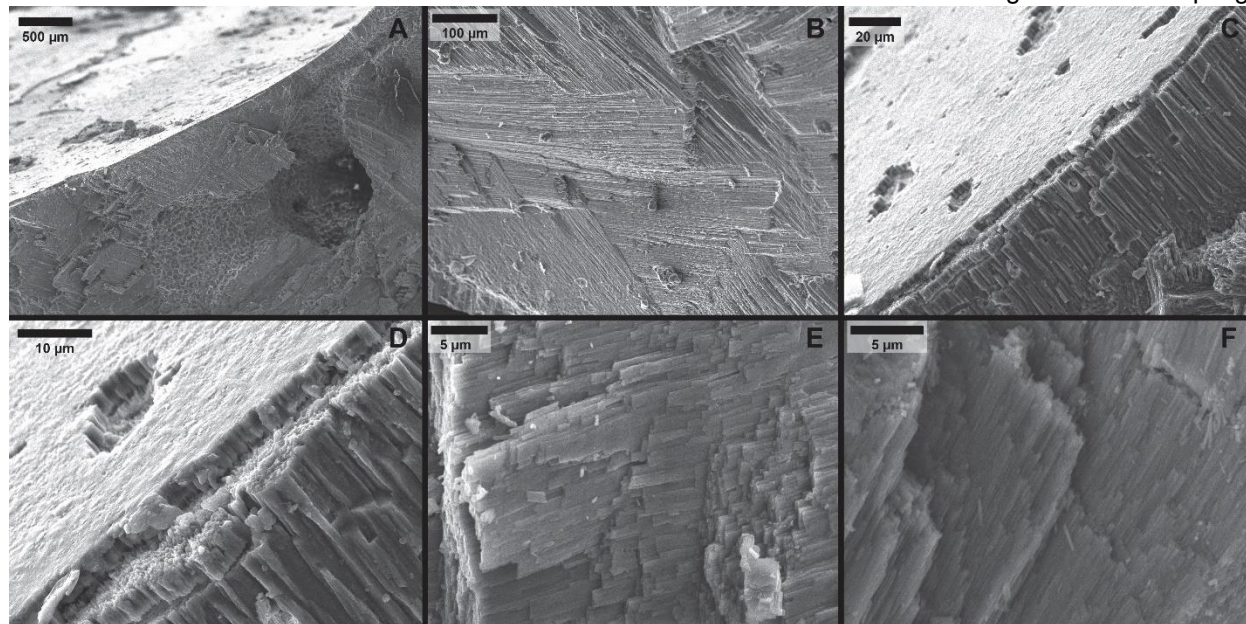
Fig S2: SEM images of fossil Campanile giganteum *shell fragments. **A**) Low (33x) magnification image of break surface of the outer edge of shell showing orientation of pristine aragonite crystals and the presence of a burrow around which aragonite is reprecipitated and mixed with detrital minerals. **B**) Medium (200x) magnification image showing the orientation of well-preserved fibrous aragonite crystals in crossed orientation. **C**) Medium (800x) magnification image of cross section through the edge of the inner aperture of the shell showing well-preserved aragonite crystals towards the inside of the shell and a thin (~10 µm) layer of preserved nacre on the inside of the shell aperture. **D**) High (2300x) magnification showing a close up of the nacre layer shown in **C** showing the preservation of nacre columns perpendicular to the inner surface of the shell aperture. **E**) High magnification (3500x) close up of well-preserved aragonite crystals in the secondary aragonite precipitated inside the shell whorl. **F**) High (4500x) magnification image of fibrous aragonite crystals demonstrating excellent preservation of the shell minerals.*

Cathodoluminscence microscopy was applied as a second method for assessing the quality of preservation of aragonite in *C. giganteum*. Cold cathodoluminescence (CL) refers to the emission of light of a sample that has been excited by an electron beam. The wavelength (color) of the emitted light contains information about the crystal lattice of the material and, as such, can be used to visualize variations in the mineralogy of the sample under investigation (Barbin, 2000). In this study, CL was applied to verify whether parts of the shells of *C. giganteum* were recrystallized or altered during the fossilization process. In case recrystallization occurred, this often results in an increase in Mn^{2+} concentrations in the shell material, which

leads to increased luminescence, or to a complete transformation of aragonite to calcite, which leads to a distinct change in the wavelength of luminescence (Barbin, 2000).

Polished longitudinal cross sections through **E1** were analyzed using a Technosyn Cold Cathodoluminscence model 8200 Mark II (CITL, Cambridge, UK) microscope equipped with an electron cathode operating between 5-6 kV with a 550-600 µA beam current. Specimens were brought into a vacuum chamber (5.5 * 10^{-5} bar) and illuminated with an electron beam with a diameter of 5 mm. Luminenscence of the sample in response to excitation by the electron beam was observed at 75x magnification. Images of luminescence were obtained through a digital camera connected to the microscope and processed using Adobe Photoshop CS2 (Adobe Systems, California, USA) to enhance brightness and contrast and visualize differences in luminescence between parts of the shell.

Excellent preservation of the shells of *C. giganteum* specimens was evident from the weak blue luminescence observed in CL images (**Fig. S5**). The absence of bright luminescence as well as the blue color of the weak luminescence observed in the samples is a clear sign that the samples of *C. giganteum* shell consist of aragonite with very little alterations or impurities. Any recrystallization to calcite would yield an orange luminescence, while impurities in the aragonite of the shell would result in brighter luminescence. The only difference that could be observed within the shell fragments of **E1** was that the secondary aragonite precipitated within the shell whorl showed a slightly brighter luminescence compared to the rest of the shell, indicating slightly elevated concentrations of trace element impurities in this part of the shell.
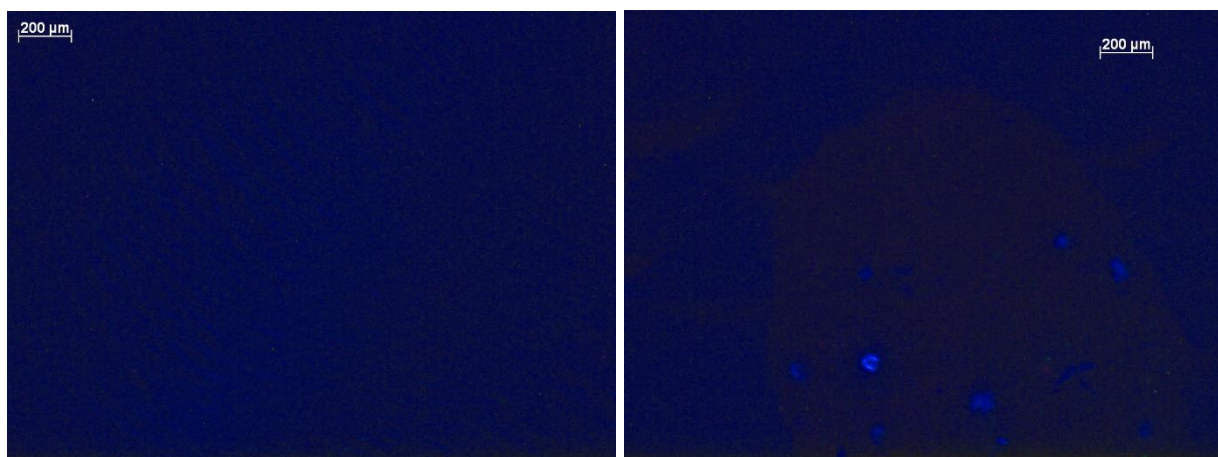
Fig S3: *CL images of shell **E1** showing, on the left, weakly luminescent parts of the columella of the shell and, on the right, slightly brighter luminescence inside the shell whorl.*

In addition to CL microscopy, growth structures in the aragonite of *C. giganteum* shells were observed using visible light microscopy. Micrographs of the growth and mineral structures of *C. giganteum* shell **E1** were visualized in regular visible and cross polarized light using a Nikon Optiphot 2 POL light microscope (Nikon Corp., Tokyo, JP) in order to reconstruct the preservation and growth direction of different parts of the shell (**Fig. S4**; see **SI_shellgrowth**). The state of preservation of aragonite in the *C. giganteum* shells was evident from the presence of original growth structures and crystal orientations that showed no sign of recrystallization. These structures allowed the direction of growth in these shells to be reconstructed which aided greatly in the alignment of records of chemical proxies measured in different parts of the shells (**SI_shellgrowth**).
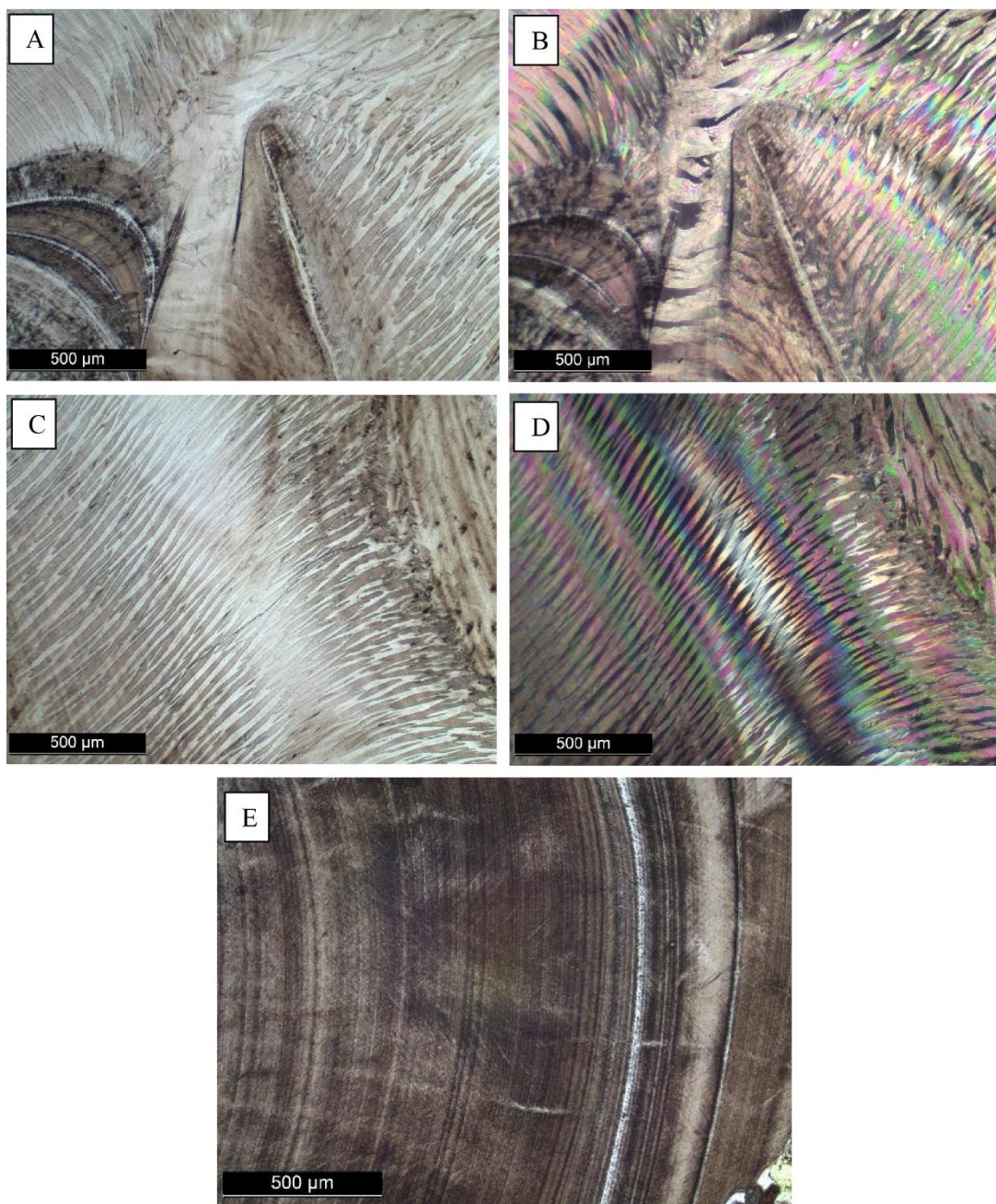
Fig S4*: Microscope pictures under normal polarized light (PPL) and crossed polarized light (XPL) showing growth lines as alternating black and white lines. The difference between crystal orientations is seem in the XPL pictures. A) PPL picture of a borderline near a whorl. B) XPL picture of a borderline near a whorl. C) PPL picture of a junction between two whorls. D) XPL picture of a junction between two whorls. E) PPL picture of a secondary whorl infill where fine laminations are seen.*

XRF mapping provided another line of evidence for examining the preservation of original aragonite in *C. giganteum* shells. Using the Bruker M4 Tornado µXRF scanner (Bruker nano GmbH, Berlin, Germany), XRF maps were created of entire longitudinal cross sections through the shells of *Campanile giganteum*. For this purpose, the Bruker M4 Tornado was operated in mapping mode (see **SI_XRF**) and allowed to

scan the entire surface of longitudinal shell cross sections to obtain semi quantitative maps of elemental distributions through the shell. Maps of Mn, Fe, Sr and Si (**Fig. S5**) show that the aragonite in *C. giganteum* shells is characterized by very low concentrations in Mn and Fe and high concentrations of Sr. The only regions of the cross section that show elevated concentrations of Fe are the places where the shell is affected by boring and where detrital material entered the bore holes. Another interesting observation is that Sr concentrations are elevated in the secondary aragonite that is deposited on the inside of the whorl of the shell. This latter observation demonstrates that the brighter luminescence in this part of the shell is indeed caused by increased concentrations of trace elements. In addition to semi-quantitative XRF mapping, quantified measurements in XRF line scans showed that the concentrations of Mn and Fe generally remain below 50 µg/g and 20 µg/g respectively. High concentrations of these elements (>200 µg/g) are generally associated with diagenetic alteration (Brand and Veizer, 1980; Al-Aasm and Veizer, 1986a), so these low concentrations attest to the excellent preservation of the *C. giganteum* shells.
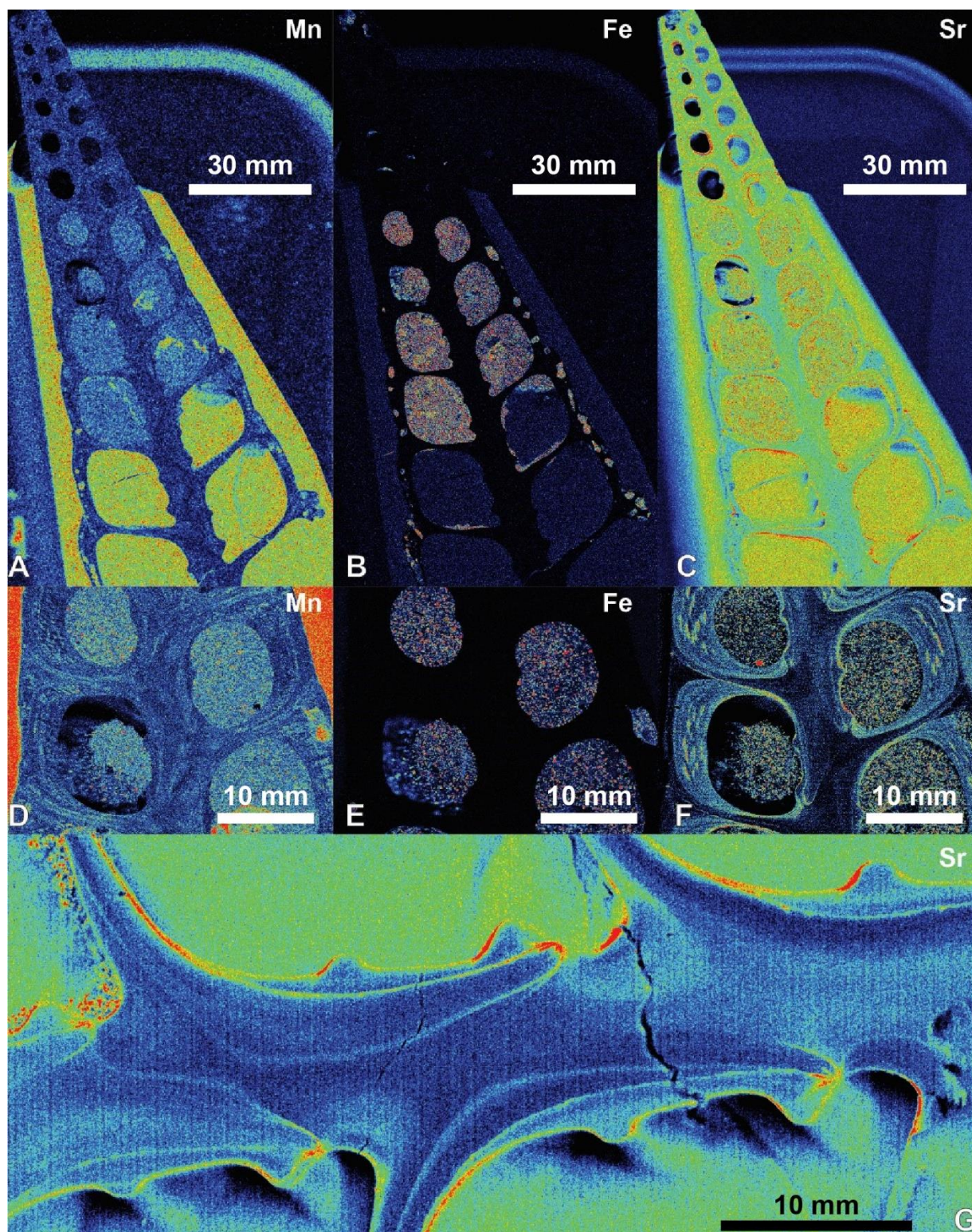
Fig. S5: *Heatmaps of elemental distributions in semi quantitative XRF maps of cross sections through the shells* C. giganteum. *Red colors show high concentrations while bluish concentrations indicate lower concentrations. A) Map of Mn distribution in cross section through shell* **E3** *showing low concentrations in the aragonite and elevated concentrations in boreholes and whorls which are filled up with sediment. B)*

*Map of Fe distribution in cross section through shell **E3** showing low concentrations in the aragonite and elevated concentrations in boreholes and whorls which are filled up with sediment. C) Map of Sr distribution in cross section through shell **E3** showing elevated concentrations in secondary aragonite precipitated on the inside of the whorl. D) Higher resolution close-up of A. E) Higher resolution close-up of B. F) Higher resolution close-up of C. G) High resolution Sr map of the columella of **E3** showing elevated Sr concentrations associated with growth layers in the shell.*

The exceptional preservation of fossil *C. giganteum* shells used in this study is evident from the presence of original nacre on the inside of the shell and original aragonite in several other parts of the shell (see **Fig. S2**). Cathodoluminescence microscopy shows that shell **E1**, which is most severely affected by boring, shows no luminescence, demonstrating that there is no evidence of recrystallization of the original aragonite in the shell (Savard et al., 1996; **Fig. S3**). Furthermore, polarized light microscopy shows that the original crystal structure of the shell is preserved (Gerhardt et al., 2000; **SI_microscopy**) and µXRF mapping demonstrates that concentrations of Mn and Fe (both associated with diagenetic recrystallization; Brand and Veizer, 1980; Al-Aasm and Veizer, 1986a) in the aragonite are very low (<100 µg/g and <50 µg/g respectively), attesting to the excellent preservation of the shell and limited neomorphism (Maliva and Dickson, 1992; Hendry et al., 1995). Both nacre and aragonite are very susceptible to diagenesis (Brand and Veizer, 1980), and the preservation of these materials over 45 Myr demonstrates the unique quality of fossil material from the Fleury-la-Rivière locality.

References

Barbin, V., 2000. Cathodoluminescence of carbonate shells: biochemical vs diagenetic process, in: Cathodoluminescence in Geosciences. Springer, pp. 303–329.

Brand, U., Veizer, J., 1980. Chemical diagenesis of a multicomponent carbonate system–1: Trace elements. Journal of Sedimentary Research 50.

Cochran, J.K., Kallenberg, K., Landman, N.H., Harries, P.J., Weinreb, D., Turekian, K.K., Beck, A.J., Cobban, W.A., 2010. Effect of diagenesis on the Sr, O, and C isotope composition of late Cretaceous mollusks from the Western Interior Seaway of North America. Am J Sci 310, 69–88. https://doi.org/10.2475/02.2010.01

Dauphin, Y., Cuif, J.P., Mutvei, H., Denis, A., 1989. Mineralogy, chemistry and ultrastructure of the external shell-layer in ten species of Haliotis with reference to Haliotis tuberculata (Mollusca: Archaeogastropoda). Bulletin of the Geological Institutions of the University of Uppsala 15, 7–37.

Gerhardt, S., Groth, H., Rühlemann, C., Henrich, R., 2000. Aragonite preservation in late Quaternary sediment cores on the Brazilian Continental Slope: implications for intermediate water circulation. Int Journ Earth Sciences 88, 607–618. https://doi.org/10.1007/s005310050291

Hendry, J.P., Ditchfield, P.W., Marshall, J.D., 1995. Two-stage neomorphism of Jurassic aragonitic bivalves; implications for early diagenesis. Journal of Sedimentary Research 65, 214–224.

Maliva, R.G., Dickson, J.A.D., 1992. The mechanism of skeletal aragonite neomorphism: evidence from neomorphosed mollusks from the upper Purbeck Formation (Late Jurassic-Early Cretaceous), southern England. Sedimentary Geology 76, 221–232. https://doi.org/10.1016/0037-0738(92)90085-6

Savard, M.M., Beauchamp, B., Veizer, J., 1996. Significance of aragonite cements around Cretaceous marine methane seeps. Journal of Sedimentary Research 66, 430–438. https://doi.org/10.1306/D4268365-2B26-11D7-8648000102C1865D

Taylor, J.D., Reid, D.G., 1990. Shell microstructure and mineralogy of the Littorinidae: ecological and evolutionary significance, in: Progress in Littorinid and Muricid Biology. Springer, pp. 199–215.